Anticipated synchronization in human EEG data: Unidirectional causality with negative phase lag

Francisco-Leandro P. Carlos,[1] Maciel-Monteiro Ubirakitan,[2,3] Marcelo Cairrão Araújo Rodrigues,[2] Moisés Aguilar-Domingo,[3,4] Eva Herrera-Gutiérrez,[5] Jesús Gómez-Amor,[4,*] Mauro Copelli,[6] Pedro V. Carelli,[6] and Fernanda S. Matias[1,†]

[1]*Instituto de Física, Universidade Federal de Alagoas, Maceió, Alagoas 57072-970 Brazil*
[2]*Grupo de Neurodinâmica, Departamento de Fisiologia e Farmacologia, Universidade Federal de Pernambuco, Recife PE 50670-901, Brazil*
[3]*Spanish Foundation for Neurometrics Development, Department of Psychophysics & Psychophysiology, 30100, Murcia, Spain*
[4]*Department of Human Anatomy and Psychobiology, Faculty of Psychology, University of Murcia, 30100 Espinardo Campus, Murcia, Spain*
[5]*Department of Developmental and Educational Psychology, Faculty of Psychology, University of Murcia, 30100 Espinardo Campus, Murcia, Spain*
[6]*Departamento de Física, Universidade Federal de Pernambuco, Recife PE 50670-901, Brazil*

(Received 5 June 2020; accepted 15 July 2020; published 18 September 2020)

Understanding the functional connectivity of the brain has become a major goal of neuroscience. In many situations the relative phase difference, together with coherence patterns, has been employed to infer the direction of the information flow. However, it has been recently shown in local field potential data from monkeys the existence of a synchronized regime in which unidirectionally coupled areas can present both positive and negative phase differences. During the counterintuitive regime, called anticipated synchronization (AS), the phase difference does not reflect the causality. Here we investigate coherence and causality at the alpha frequency band ($f \sim 10$ Hz) between pairs of electroencephalogram (EEG) electrodes in humans during a GO/NO-GO task. We show that human EEG signals can exhibit anticipated synchronization, which is characterized by a unidirectional influence from an electrode A to an electrode B, but the electrode B leads the electrode A in time. To the best of our knowledge, this is the first verification of AS in EEG signals and in the human brain. The usual delayed synchronization (DS) regime is also present between many pairs. DS is characterized by a unidirectional influence from an electrode A to an electrode B and a positive phase difference between A and B which indicates that the electrode A leads the electrode B in time. Moreover we show that EEG signals exhibit diversity in the phase relations: the pairs of electrodes can present in-phase, antiphase, or out-of-phase synchronization with a similar distribution of positive and negative phase differences.

DOI: 10.1103/PhysRevE.102.032216

I. INTRODUCTION

The extraordinary ability of humans to model and predict facts is one of the prerequisites for both action and cognition. These capacities emerge from the various synchronous rhythms generated by the brain [1,2], which represent a core mechanism for neuronal communication [3]. In particular, phase synchronization [4] has been related to selective attention [5,6], large-scale information integration [7], and memory processes [8,9]. Despite enormous evidence of zero-lag synchronization in the brain [2], there is a growing number of studies reporting nonzero phase differences between synchronized brain areas [6,9–13]. It has been assumed that phase diversity plays an important role in fast cognitive processes [14].

In many situations the phase, together with coherence patterns, has been employed to infer the direction of the information flow [10,15–19]. The assumption is typically that the phase difference reflects the transmission time of neural activity. However, this assumed relationship is not theoretically justified [20]. In particular, during special synchronized regimes, the phase difference does not reflect the causality [21–25].

It has been shown that a monkey performing a cognitive task can present unidirectional influence from a cortical region A to another region B with a negative phase difference between the two areas [21–23]. This means that the receiver region B can lead the activity of A. For example, it has been observed that during the waiting period of a GO/NO-GO task, a macaque monkey presents unidirectional causality from the somatosensory cortex to the motor cortex with a negative phase [21,23]. A similar apparent incongruence has been verified between the prefrontal cortex (PFC) and posterior parietal cortex (PPC) in monkeys performing a working memory task [22]. The information flows from the PPC to the PFC, but the activity of the PFC leads the activity of the PPC by 2.4 to 6.5 ms.

These experimental results have been compared to a model of two unidirectionally coupled neuronal populations [23]. The phase difference between the sender and the receiver population can be controlled by the inhibitory synaptic conductance in the receiver population [23] or by the amount

*Deceased.
†fernanda@fis.ufal.br

of external noise at the receiver [26]. By construction, the information flow is always from the sender to the receiver population, but the receiver can lead the sender, which is characterized by a negative phase difference. In other words, the sender lags behind the receiver. Results were corroborated using the statistical permutation quantifiers in the multiscale entropy causality plane [27]. This counterintuitive regime has been explained in the light of anticipated synchronization (AS) ideas [23,28].

The anticipatory synchronization can be a stable solution of two dynamical systems coupled in a sender-receiver configuration, if the receiver is also subjected to a negative delayed self-feedback [28–34]:

$$\dot{\mathbf{S}} = \mathbf{f}(\mathbf{S}(t)),$$
$$\dot{\mathbf{R}} = \mathbf{f}(\mathbf{R}(t)) + \mathbf{K}[\mathbf{S}(t) - \mathbf{R}(t - t_d)]. \quad (1)$$

$\mathbf{S}$ and $\mathbf{R} \in \mathbb{R}^n$ are dynamical variables, respectively, representing the sender and the receiver systems. $\mathbf{f}$ is a vector function which defines each autonomous dynamical system, $\mathbf{K}$ is the coupling matrix, and $t_d > 0$ is the delay in the receiver's negative self-feedback. In such a system, $\mathbf{R}(t) = \mathbf{S}(t + t_d)$ is a solution of the system, which can be easily verified by direct substitution in Eq. (1). AS has been observed in excitable models driven by white noise [35] and chaotic systems [28,31], as well as in experimental setups with semiconductor lasers [36,37] and electronic circuits [38].

AS has also been observed when the self-feedback was replaced by parameter mismatches [39–43], inhibitory dynamical loops [23,44–46], and noise at the receiver [26]. It has been suggested that AS can emerge when the receiver's dynamics is faster than the sender's [26,46–48]. Furthermore, unidirectionally coupled lasers reported both regimes: AS and the usual delayed synchronization (DS, in which the sender predicts the activity of the receiver), depending on the difference between the transmission time and the feedback delay time [37,49]. The two regimes were observed to have the same stability of the synchronization manifold in the presence of small perturbations due to noise or parameter mismatches [37]. Neuron models can also present a transition from positive to negative phase differences (from DS to AS) depending on coupling parameters [23,26,44,45]. Therefore, the study of anticipatory regimes in biological systems (not manmade) has been receiving more attention recently [50–53].

Here we employ spectral coherence and Granger causality (GC) measures to infer the direction of influence, as well as the phase difference between electrodes of the EEG from 11 subjects. We verify, for all subjects, the existence of coherent activity in the alpha band ($f \sim 10$ Hz) between pairs of electrodes. We also show that many of these pairs exhibit a unidirectional influence from one electrode to another and a phase difference that can be positive or negative. In Sec. II and Appendix we describe the experimental paradigm and EEG processing and analysis. In Sec. II we report our results, showing that when we consider all the unidirectionally coupled pairs we verify that there is a diversity in the phase relation: they exhibit in-phase, antiphase, or out-of-phase synchronization with a similar distribution of positive and negative phase differences (DS and AS, respectively). Concluding remarks and brief discussion of the significance of our findings for neuroscience are presented in Sec. III.

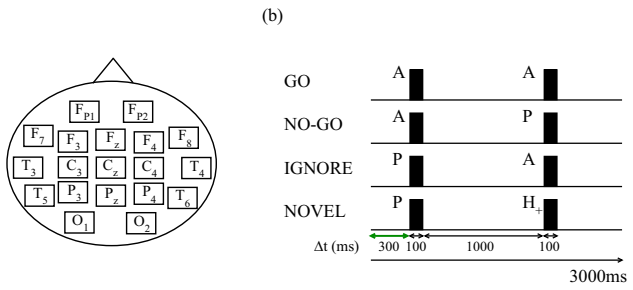

FIG. 1. Experimental paradigm. (a) 10/20 system of EEG electrode placement employed in the experiments. (b) GO/NO-GO task based on three types of stimulus with images of animals (A), plants (P), and people (H_+). After a waiting window of 300 ms, two stimulus were presented for 100 ms, with a 1000 ms interstimulus interval. If both stimulus are animals (AA) the participant should press a button as quickly as possible (see Appendix for more details). Here we analyzed the 300 ms before the stimulus onset.

II. RESULTS

The experiment consists of 400 trials of a GO/NO-GO task. In each trial a pair of stimuli were presented after a waiting window of 300 ms, which is the important interval for our analysis [see the green arrow in Fig. 1(b)]. Depending on the combination of stimuli, participants should press a button or not. Oscillatory main frequency, synchronized activity, and directional influence were estimated by the power, coherence, phase difference, and Granger causality spectra as reported in Matias *et al.* [23] (see Appendix for more details).

Synchronization between electrodes l and k can be characterized by a peak in the coherence spectrum $C_{lk}(f_{\text{peak}})$. The phase difference $\Delta\Phi_{l-k}$ at the peak frequency f_{peak} provides the time delay τ_{lk} between the electrodes. The direction of influence is given by the Granger causality spectrum. Whenever an electrode l strongly and asymmetrically G-causes k, we refer to l as the sender (S) and to k as the receiver (R), and the link between l and k is considered a unidirectional coupling from l to k (S $\rightarrow$ R). After determining which electrode is the sender and which one is the receiver we analyze the sign of $\Delta\Phi_{S-R}$ to determine the synchronized regime. Unless otherwise stated we analyze only the unidirectionally connected pairs.

A. Delayed synchronization (DS): Unidirectional causality with positive phase lag

Typically when a directional influence is verified from A to B, a positive time delay is expected, indicating that A's activity temporally precedes that of B [10,54]. This positive time delay characterizes the intuitive regime called delayed synchronization (DS, or also retarded synchronization) in which the sender is also the leader [37]. In neuronal models the time delay between A and B can reflect the characteristic timescale of the synapses between A and B but can also be modulated by local properties of the receiver region B [23,26].

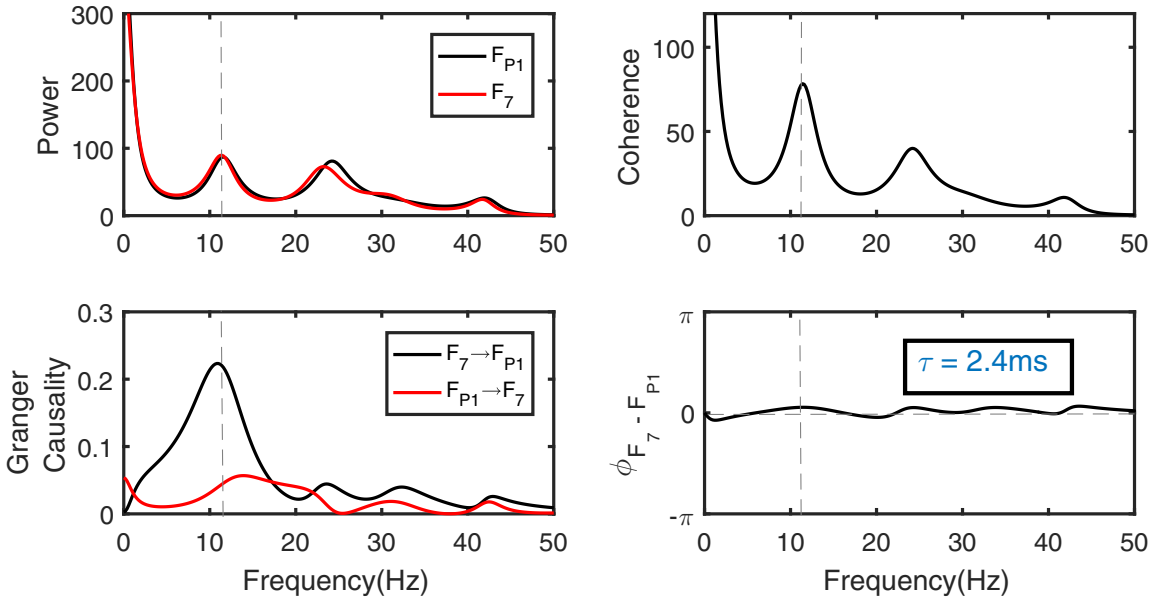

FIG. 2. Unidirectional causality with positive phase lag characterizes the delayed synchronization regime (DS). Power, coherence, Granger causality, and phase spectra between electrodes F_7 and F_{P1} for volunteer 439. The pair is synchronized with main frequency $f_{\text{peak}} = 11.4$ Hz (given by the peak of the coherence, gray dashed lines). The Granger causality peak around f_{peak} reveals a directional influence from site F_7 to F_{P1}, and the phase difference at the main frequency $\Delta\Phi_{F_7-F_{P1}}(f_{\text{peak}}) = 0.1727$ rad shows that F_7 leads F_{P1} (with an equivalent time delay $\tau = 2.4$ ms).

In Fig. 2 we show an example of DS between the sites F_7 and F_{P1} for volunteer 439. Power and coherence spectra present a peak at $f_{\text{peak}} = 11.4$ Hz. At this frequency, the activity of F_7 G-causes F_{P1}, but not the other way around. The positive sign of the phase $\Delta\Phi_{F_7-F_{P1}}(f_{\text{peak}}) = 0.1727$ rad indicates that the sender electrode F_7 leads the receiver electrode F_{P1} with a positive time delay $\tau = 2.4$ ms.

B. Anticipated synchronization (AS): Unidirectional causality with negative phase lag

Despite the fact that phase differences and coherence patterns have been employed to infer the direction of the information flux [10,15–19], our results imply that if we consider only the coherence and phase lag we could infer the

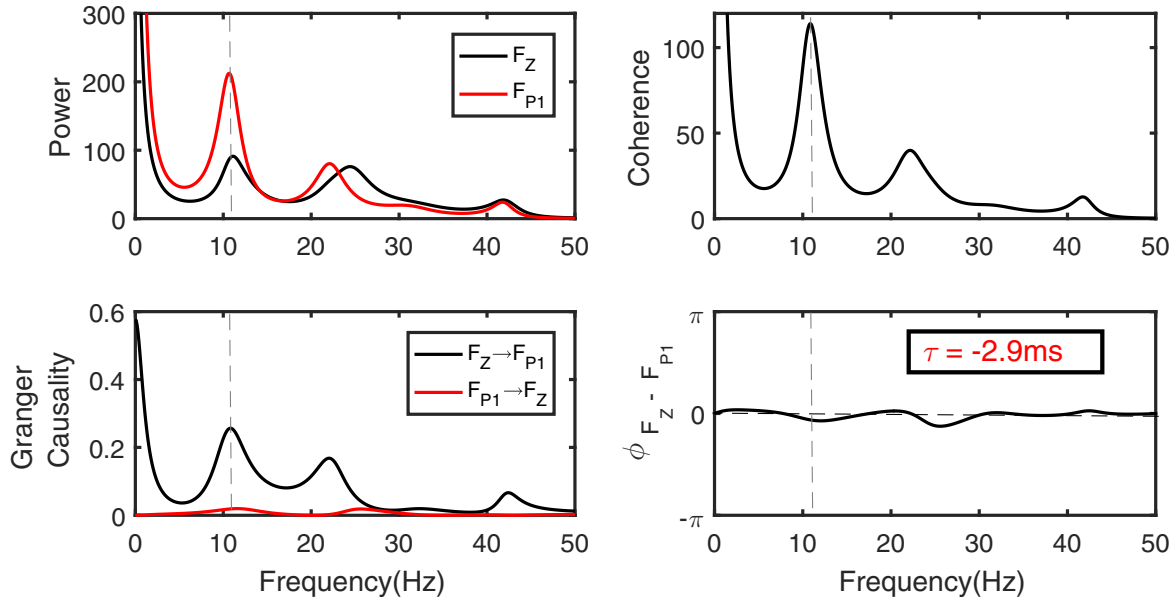

FIG. 3. Unidirectional causality with negative phase lag characterizes anticipated synchronization (AS). Power, coherence, Granger causality, and phase spectra between sites F_Z and F_{P1} for volunteer 439. The electrodes are synchronized with main frequency $f_{\text{peak}} = 10.8$ Hz (given by the peak of the coherence, gray dashed lines). The Granger causality peak around f_{peak} reveals a directional influence from site F_Z to F_{P1}. F_Z G-causes F_{P1}, but the negative phase difference at the main frequency $\Delta\Phi_{F_Z-F_{P1}}(f_{\text{peak}}) = -0.1969$ rad (which is equivalent to a time delay $\tau = -2.9$ ms) indicates that F_{P1} leads F_Z in time.

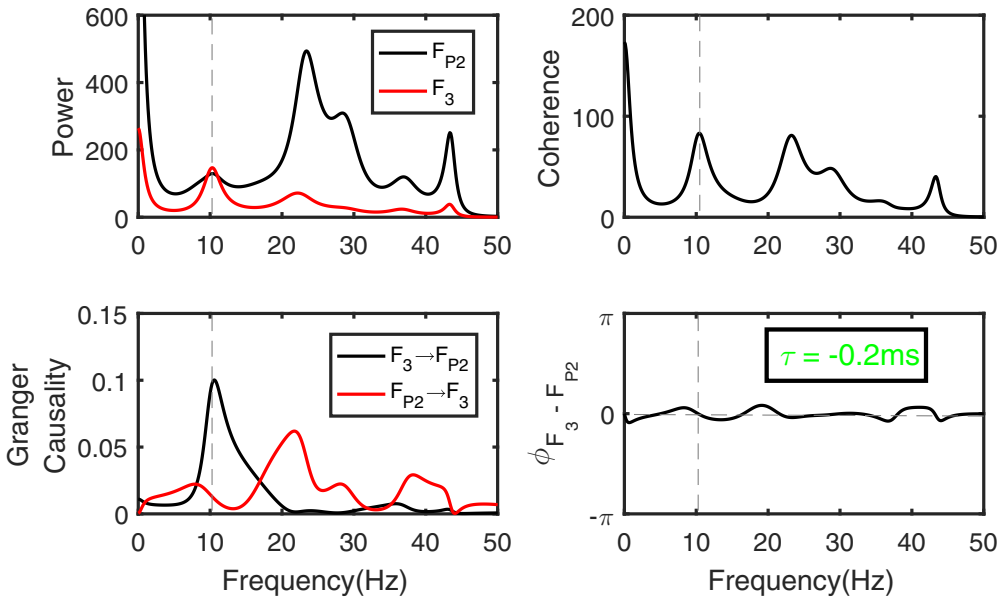

FIG. 4. Unidirectional causality with zero-lag synchronization (ZL, defined by $\Delta\Phi \simeq 0$). Power, coherence, Granger causality, and phase spectra between electrodes F_3 and F_{P2} for volunteer 439. Sites are synchronized with main frequency (given by the peak of the coherence, brown dashed lines) $f_{\text{peak}} = 10.4$ Hz. The Granger causality peak around f_{peak} indicates that site F_3 unidirectionally influences F_{P2}. The time delay between both is almost zero $\tau = -0.2$ ms [$\Delta\Phi_{F_3-F_{P2}}(f_{\text{peak}}) = -0.0164$ rad].

wrong direction of influence between the involved pairs. Such a counterintuitive regime exhibiting unidirectionally causality with negative phase difference has first been reported in the brain as a mismatch between causality and the sign of the phase difference in the local field potential of macaque monkeys during cognitive tasks [21,22]. Afterwards, it has been reported that the apparent paradox could be explained in the light of anticipated synchronization ideas [23]. Here we show that human EEG signals can also present unidirectional influence with negative phase lag. As far as we know, this is the first evidence of AS in human EEG data.

An example of anticipated synchronization between EEG electrodes is shown in Fig. 3. The sites F_Z and F_{P1} exhibit a peak at the alpha band in the power and coherence spectra for $f_{\text{peak}} = 10.8$ Hz (Fig. 3) for volunteer 439. The Granger causality spectra presents a peak from F_Z to F_{P1} but not

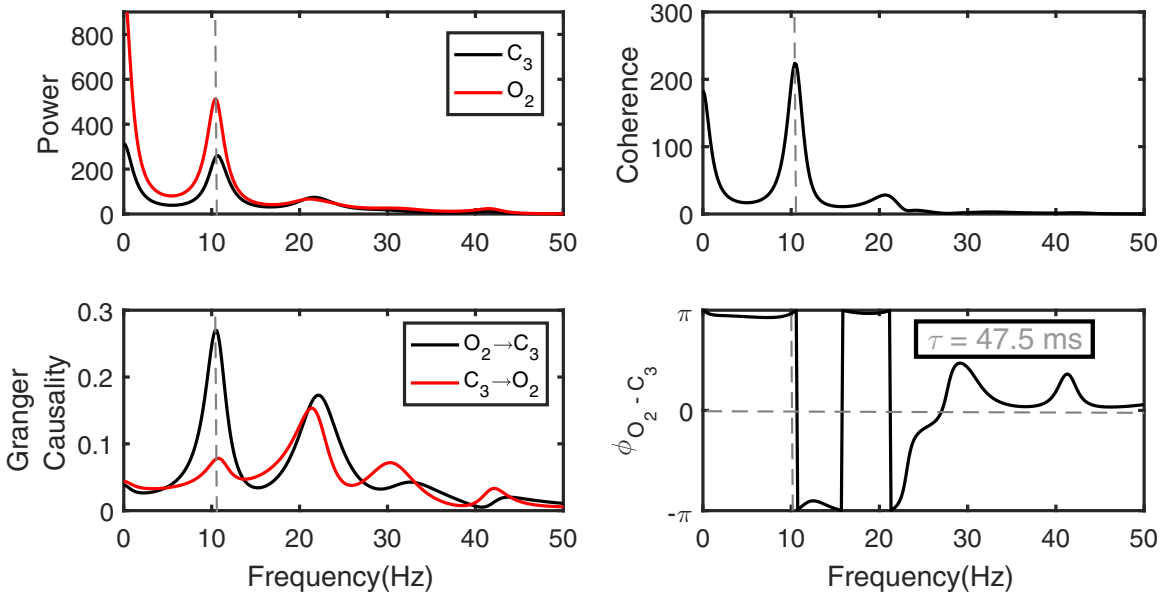

FIG. 5. Unidirectional causality with antiphase synchronization (AP, defined by $\Delta\Phi \simeq \pm\pi$). Power, coherence, Granger causality, and phase spectra between electrodes O_2 and C_3 for volunteer 439. The activity of the electrodes are synchronized with main frequency $f_{\text{peak}} = 10.4$ Hz (gray dashed lines). The Granger causality peak around f_{peak} reveals a directional influence from O_2 to C_3, and the phase spectrum shows that $\Delta\Phi_{O_2-C_3}(f_{\text{peak}}) = 3.1031$ rad (which provides $\tau = 47.5$ ms).

in the opposite direction, indicating that F_Z G-causes F_{P1} at $f_{\text{peak}} = 10.8$ Hz. However, the negative sign of the angle $\Delta\Phi_{F_Z-F_{P1}}(f_{\text{peak}}) = -0.1969$ rad indicates that the activity of F_Z lags behind the activity of F_{P1}. The time delay associated with $\Delta\Phi_{F_Z-F_{P1}}(f_{\text{peak}})$ is $\tau = -2.9$ ms.

It is worth mentioning that for linear phase responses, which is the case for a simple monochromatic sinusoidal function, the phase delay and the group delay (defined by the derivative of phase with respect to frequency) are identical. In this case, both phase and group delays may be interpreted as the actual time delay between the signals. For time series that are synchronized in a broad frequency band, the group delay could be useful to estimate the time difference between the signals. Indeed, a negative group delay has been associated with anticipatory dynamics [55–57], and it is comparable to the time difference obtained by the cross-correlation function [55]. Here we verified that some AS pairs present both negative phase delay and negative group delay (as in the example shown in Fig. 3). However, this is not the case for all AS pairs in the analyzed data. We have found all possible combinations for the signs of phase and group delays for both DS and AS. A further investigation of the relation between phase delay and group delay in brain signals is out of the scope of this paper and should be done elsewhere.

C. Zero-lag synchronization (ZL)

Zero-lag (ZL) synchronization has been widely documented in experimental data since its first report in the cat visual cortex [58]. It has been related to different cognitive functions such as perceptual integration and the execution of coordinated motor behaviors [3,7,59,60]. Despite many models showing that bidirectional coupling between areas promotes ZL synchronization [61,62], it is also possible to have ZL between unidirectional connected populations [23,26,45]. In these systems, nonlinear properties of the receiver region can compensate for characteristic synaptics delays, and the two systems synchronize at zero phase.

We consider zero lag whenever $|\Delta\Phi_{S-R}(f_{\text{peak}})| < 0.1$ rad. In Fig. 4 we show power, coherence, Granger causality and phase spectra between electrodes F_3 and F_{P2} for volunteer 439. These sites are synchronized with main frequency $f_{\text{peak}} = 10.4$ Hz and $\Delta\Phi_{F_3-F_{P2}}(f_{\text{peak}}) = -0.0164$ rad, which provides $\tau = -0.2$ ms.

D. Antiphase synchronization

Participants can also exhibit antiphase synchronization between electrodes. We define antiphase synchronization (AP) when $\pi - 0.1 < |\Delta\Phi_{S-R}(f_{\text{peak}})| < \pi + 0.1$ rad. In Fig. 5 we show power, coherence, Granger causality, and phase spectra between electrodes O_2 and C_3 for volunteer 439. The site O_2 G-causes C_3, and the time delay between them is $\tau = 47.5$ ms, which is almost half of a period for $f_{\text{peak}} = 10.4$ Hz.

E. Phase relation diversity across pairs and subjects

Reliable phase relation diversity is a general property of brain oscillations. It has been reported on multiple spatial scales, ranging from very small spatial scale (interelectrode distance <900 mm) in macaques [6,9] to a large spatial scale

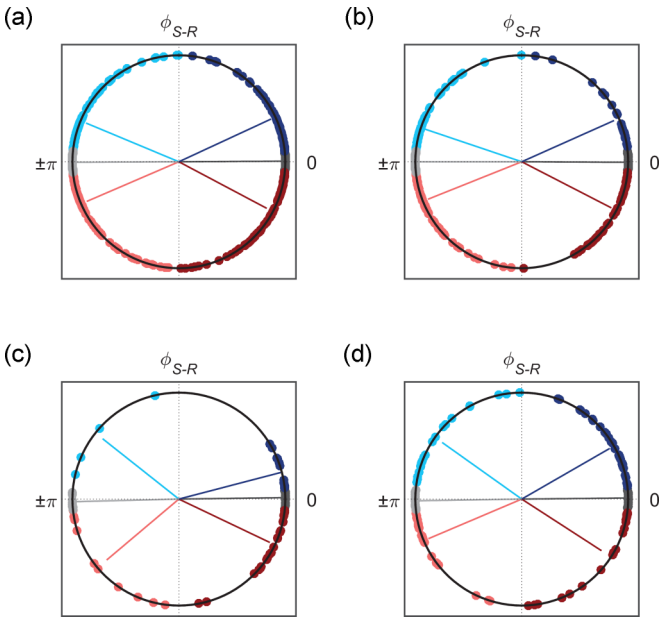

FIG. 6. Circular phase differences distribution. The pairs are separated into six groups relative to their phase-synchronization regime: zero-lag (ZL, dark gray), antiphase (AP, light gray), delayed synchronization in the first quadrant (DS(1), dark blue), delayed synchronization in the second quadrant [DS(2), light blue], anticipated synchronization in the fourth quadrant [AS(1), dark red], and anticipated synchronization in the third quadrant [AS(2), light red]. (a) Phase of all 686 unidirectionally connected pairs: (b) 430 pairs showing back-to-front influence, (c) 90 pairs within lateral flux, (d) 166 pairs presenting front-to-back influence.

(using magnetoencephalography) in humans [63]. However, the functional significance of phase relations in neuronal signals is not well defined. It has been hypothesized that it may support effective neuronal communication by enhancing neuronal selectivity and promoting segregation of multiple information streams [14].

Considering the 19 electrodes per subject, the number of analyzed pairs is 171 for each volunteer, which corresponds to 1881 pairs in total. Among these pairs, 1394 presented a peak in the coherence spectrum at the alpha band. Regarding the Granger causality spectra, 686 pairs presented an unidirectional influence and 358 a bidirectional influence. In Fig. 6(a) we show the phase-difference distribution of all 686 unidirectionally connected pairs for all volunteers in a circular plot. In Figs. 6(b), 6(c), and 6(d) we show all the pairs separated by the direction of influence: from the back to the front (430), lateral flux (90), and from the front to the back (166), respectively. The colors represent the four different synchronized regimes mentioned before: DS [blue for positive phase: $0.1 < \Delta\Phi_{S-R}(f_{\text{peak}}) < \pi - 0.1$ rad], AS [red for negative phase: $-\pi + 0.1 < \Delta\Phi_{S-R}(f_{\text{peak}}) < -0.1$ rad], ZL [dark gray for close to zero-phase: $|\Delta\Phi_{S-R}(f_{\text{peak}})| <$ 0.1 rad] and AP [light gray for phase close to $\pm\pi$: $\pi - 0.1 < |\Delta\Phi_{S-R}(f_{\text{peak}})| < \pi + 0.1$ rad]. We have also separated the DS and AS regimes into two different subcategories: DS(1) for phase in the first quadrant (dark blue), DS(2) for phase in the second quadrant (light blue), AS(1) for phase in the fourth quadrant (dark red), and AS(2) for phase in the third quadrant

TABLE I. Number of unidirectionally connected pairs for all subjects together: separated by phase-synchronization regime along the lines and by the direction of influence along the columns.

Total	Unidirectional 686	Back-to-front 430	Lateral 90	Front-to-back 166
ZL	93	39	25	29
DS(1)	77	25	14	38
AS(1)	99	51	27	21
AP	174	135	11	28
DS(2)	108	83	4	21
AS(2)	135	97	9	29

(light red). The numbers of pairs in each situation are shown in Table I and in Fig. 7.

The total number of synchronized and unidirectionally connected pairs varies among volunteers, as well as the distribution of phases. All subjects present DS, AS, ZL, and AP pairs [see Fig. 7(b)]. However, one subject does not present AS(1). All subjects present back-to-front, lateral and front-to-back influence and more pairs with back-to-front than front-to-back direction of influence. Considering only the back-to-front pairs, there are more AP than ZL synchronized regimes. This is also true if we compare all pairs in the second and third quadrant [AP, DS(2), and AS(2)] with the ones in the first and fourth [ZL, DS(1), AS(1)].

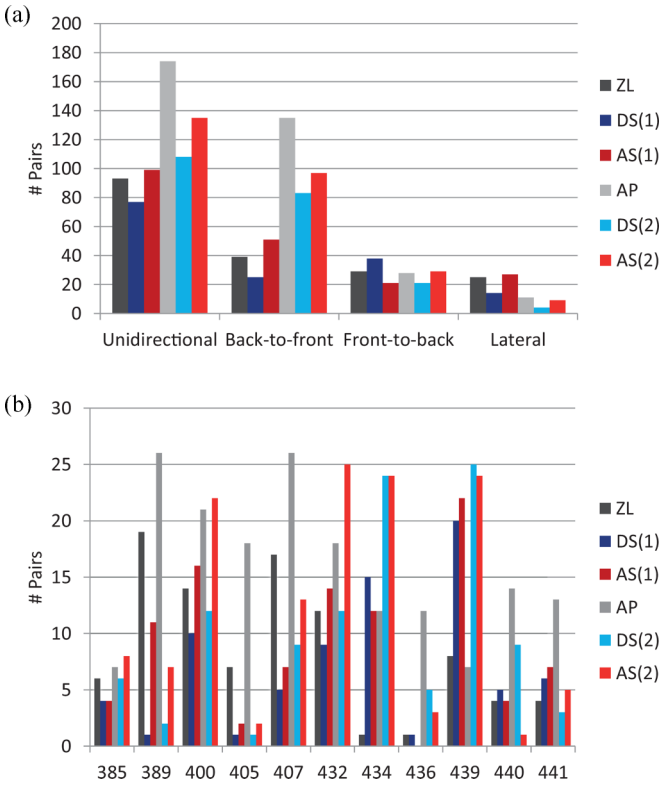

FIG. 7. Histograms for number of pairs in each synchronized regime. The colors indicate phase-synchronization regime. (a) Electrode pairs are separated by direction of influence: all unidirectional pairs, back-to-front influence, front-to-back, and lateral direction. (b) All unidirectional pairs separated per volunteer.

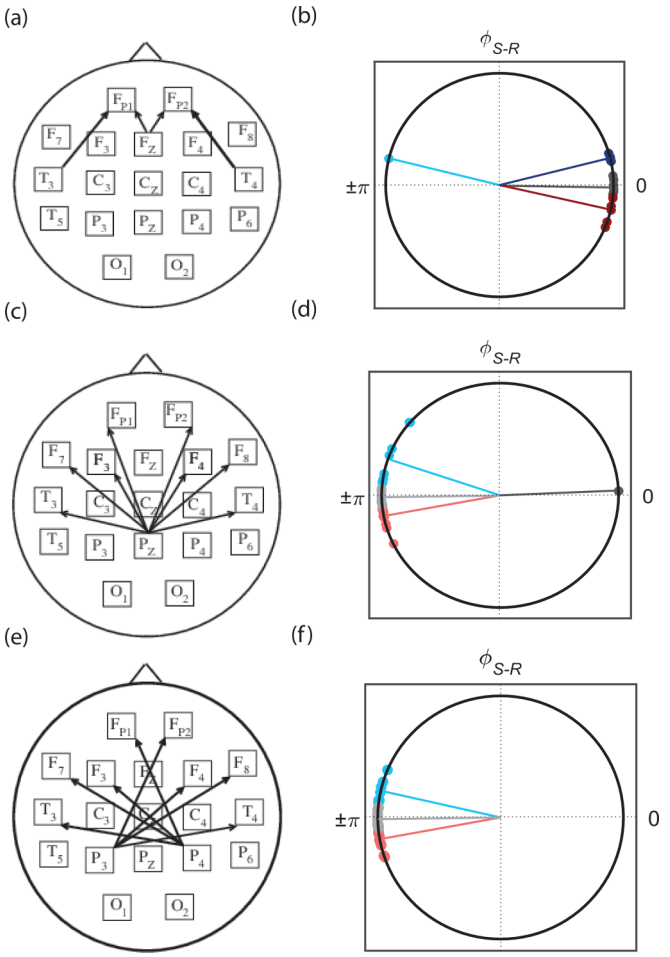

FIG. 8. Illustrative examples of unidirectionally connected pairs and their phase relations. (a, b) Example of pairs with the majority of phase differences in the first and the fourth quadrants [ZL, DS(1), AS(1)]: $F_Z \rightarrow F_{P1}$, $F_Z \rightarrow F_{P2}$, $T_3 \rightarrow F_{P1}$ and $T_4 \rightarrow F_{P2}$. (c–f) Example of pairs with the majority of phase differences in the second and the third quadrants [AP, DS(2), AS(2)]. P_Z, P_3, and P_4 are well-connected senders. All the chosen pairs are synchronized with same direction of influence for at least four subjects.

As illustrative examples, in Fig. 8 we show the direction of influence between some pairs that have the same unidirectional back-to-front Granger for at least four subjects and their respective phases. Almost all pairs that have the electrodes P_Z, P_3, and P_4 as the sender present phases close to antiphase [AP, DS(2), AS(2)], whereas almost all the pairs in which the sender is F_Z, T_3, or T_4 are synchronized close to zero lag [ZL, DS(1), AS(1)].

Regarding back-to-front influences, no pair presented the same Granger causal relation for nine or more subjects. Three pairs exhibited the same unidirectional relation for eight volunteers: $P_Z \rightarrow F_7$, $P_3 \rightarrow F_{P2}$, $O_1 \rightarrow F_4$; the other three pairs presented the same unidirectional relation for seven subjects: $P_3 \rightarrow F_4$, $P_3 \rightarrow F_8$, $O_1 \rightarrow F_{P2}$. Ten pairs had the same Granger causal relation for six volunteers: $F_Z \rightarrow F_{P1}$, $P_3 \rightarrow F_{P1}$, $P_3 \rightarrow F_3$, $C_Z \rightarrow F_8$, $C_Z \rightarrow T_3$, $C_4 \rightarrow F_{P1}$, $C_4 \rightarrow F_7$, $C_4 \rightarrow F_3$, $O_1 \rightarrow F_{P1}$, $O_2 \rightarrow F_4$. All these 16 pairs had none or only one other subject presenting the opposite

direction of the Granger causality. Out of these 16 pairs, only $F_Z \rightarrow F_{P1}$ is mostly synchronized close to ZL as shown in Figs. 6(a) and 6(b), and all the others are mostly synchronized close to AP as in Figs. 6(c)–6(f).

III. CONCLUSION

We show that human EEG can simultaneously present unidirectional causality and diverse phase relations between electrodes. Our findings suggest that the human brain can operate in a dynamical regime where the information flow and relative phase lag have opposite signs. To the best of our knowledge this is the first evidence of unidirectional influence accompanied by negative phase differences in EEG data. This counterintuitive phenomenon has been previously reported as anticipated synchronization in monkey LFP [21–23], in neuronal models [34,35,41,43,44], and in physical systems [36–40]. Therefore, we propose that this is the first verification of anticipated synchronization in EEG signals and in human brains.

Studies estimating the actual brain connectivity using data from EEG signals should consider many relevant issues such as Ref. [64]: the importance of common reference in EEG to estimate phase differences [20] and the effects of volume conduction for source localization [65,66]. Our findings suggest that it is also important to take into account the possible existence of AS in connectivity studies and separately analyze causality and phase relations. It is worth mentioning that it has been shown that for enough data points the Granger causality is able to distinguish AS and DS regimes [24]. However, for very well-behaved time series the reconstruction of the connectivity can be confused by the phase [25].

Our results open important avenues for investigating how neural oscillations contribute to the neural implementation of cognition and behavior as well as for studying the functional significance of phase diversity [6,14]. Future works could investigate the relation between anticipated synchronzation in brain signals and anticipatory behaviors [51] such as anticipation in human-machine interaction [52] and during synchronized rhythmic action [53]. It is also possible to explore the relation between consistent phase differences and behavioral data such as learning rate, reaction time, and task performance during different cognitive tasks. Neuronal models have shown that spike-timing dependent plasticity and the DS-AS transition together could determine the phase differences between cortical-like populations [45]. However, experimental evidence for the relation between learning and negative phase differences is still lacking.

We also suggest that our study can be potentially interesting for future research on the relation between inhibitory coupling, oscillations, and communication between brain areas. On the one hand, inhibition is considered to play an important role to establish the oscillatory alpha activity, in particular, allowing selective information processes [67]. On the other hand, according to the anticipated synchronization in neuronal populations model presented in Ref. [23], a modification of the inhibitory synaptic conductance at the receiver population can modulate the phase relation between sender and receiver, eventually promoting a transition from DS to AS. Therefore, we suggest that the inhibition at the receiver region can control the phase difference between cortical areas, which has been hypothesized to control the efficiency of the information exchange between these areas, via communication through coherence [3,12].

ACKNOWLEDGMENTS

The authors thank CNPq (Grants No. 432429/2016-6, No. 425329/2018-6, No. 301744/2018-1), CAPES (Grants No. 88881.120309/2016-01, No. 23038.003382/2018-39), FACEPE (Grants No. APQ-0642-1.05/18, No. APQ-0826-1.05/15), FAPEAL, UFAL and UFPE for financial support. This paper was produced as part of the activities of Research, Innovation and Dissemination Center for Neuromathematics (Grant No. 2013/07699-0, S. Paulo Research Foundation FAPESP).

APPENDIX

1. Subjects

We analyzed data from 11 volunteers (10 women, one man, all right-handed) who signed to indicate informed consent to participate in the experiment. The youngest was 32 years old, and the oldest 55 years old (average 45.7 and standard deviation 7.8). All subjects were evaluated by both a psychiatrist and psychologist. Exclusion criteria were the following: perinatal problems, cranial injuries with loss of consciousness and neurological deficit, history of seizures, medication or other drugs 24 h before the recording, presence of psychotic symptoms in the 6 months prior the study, and the presence of systemic and neurological diseases. The experiment was not specifically designed to investigate the phenomena of anticipated synchronization in humans and the data analyzed here were first analyzed in Ref. [68]. The entire experimental protocol was approved by the Commission of Bioethics of the University of Murcia (UMU, project: Subtipos electrofisiológicos y mediante estimulación eléctrica transcraneal del Trastorno por Déficit de Atención con o sin Hiperactividad).

2. EEG recording

The electroencephalographic data recordings were carried out at the Spanish Foundation for Neurometrics Development (Murcia, Spain) center using a Mitsar 201M amplifier (Mitsar Ltd), a system of 19 channels with auricular reference. Data were digitized at a frequency of 250 Hz. The electrodes were positioned according to the international 10-20 system using conductive paste (ECI ELECTRO-GEL). Electrode impedance was kept <5 KΩ. The montage [Fig. 1(a)] include three midline sites (F_Z, C_Z, and P_Z) and eight sites over each hemisphere (F_{P1}/F_{P2}, F_7/F_8, F_3/F_4, T_3/T_4, C_3/C_4, P_3/P_4, T_5/T_6, and O_1/O_2). The acquisition was realized with WinEEG software (version 2.92.56). EEG epochs with excessive amplitude (>50 μV) were automatically deleted. Finally, the EEG was analyzed by a specialist in neurophysiology to reject epochs with artifacts.

3. Experimental task

The EEG data were recorded while subjects performed a GO/NO-GO task (also called a visual continuous performance task, VCPT). Participants sat in an ergonomic chair

1.5 m away from a 17-inch plasma screen. Psytask software (Mitsar Systems) was used to present the images. The VCPT consists of three types of stimuli: 20 images of animals (A), 20 images of plants (P), and 20 images of people of different professions (H_+). Whenever H_+ was presented, a 20 ms-long artificial sound tone frequency was simultaneously produced. The tone frequencies range from 500 to 2500 Hz, in intervals of 500 Hz. All stimuli were of equal size and brightness.

In each trial a pair of stimuli were presented after a waiting window of 300 ms, which is the important interval for our analysis [see the green arrow in Fig. 1(b)]. Each stimulus remains on the screen for 100 ms, with a 1000 ms interstimulus interval. Four different kinds of pairs of stimuli were employed: AA, AP, PP, and PH_+. The entire experiment consists in 400 trials (the four kinds of pairs were randomly distributed, and each one appeared 100 times). The continuous set occurs when A is presented as the first stimulus, so the subject needed to prepare to respond. An AA pair corresponds to a GO task, and the participants are supposed to press a button as quickly as possible. An AP pair corresponds to a NO-GO task, and the participants should suppress the action of pressing the button. The discontinuous set, in which P is first presented, indicates that one should not respond (independently of the second stimuli). IGNORE task occurred with PP pairs and NOVEL when PH_+ pairs appeared. Participants were trained for about 5 min before beginning the experimental trials. They rested for a few minutes when they reached the halfway point of the task. The experimental session lasted $\sim$30 min.

4. EEG processing and analysis

The power, coherence, Granger causality, and phase difference spectra were calculated following the methodology reported in Matias *et al.* [23] using the autoregressive modeling method (MVAR) implemented in the MVGC Matlab toolbox [69]. Data were acquired while participants were performing the GO/NO-GO visual pattern discrimination described before. Our analysis focuses on 30 000 points representing the waiting window of 400 trials ending with the visual stimulus onset [green arrow in Fig. 1(b)]. This means that in each trial, the 300-ms prestimulus interval consists of 75 points with a 250-Hz sample rate.

The preprocess of the multitrial EEG time series consists in detrending, demeaning, and normalization of each trial. Respectively, it means to subtract from the time series the best-fitting line, the ensemble mean, and divide it by the temporal standard deviation. After these processes each single trial can be considered as produced from a zero-mean stochastic process. In order to determine an optimal order for the MVAR model we obtained the minimum of the Akaike Information Criterion (AIC) [70] as a function of model order. The AIC dropped monotonically with increasing model order up to 30.

For each pair of sites (l, k) we calculated the spectral matrix element $S_{lk}(f)$ [21,71], from which the coherence spectrum $C_{lk}(f) = |S_{lk}|^2/[S_{ll}(f)S_{kk}(f)]$ and the phase spectrum $\Delta\Phi_{l-k}(f) = \tan^{-1}[\mathrm{Im}(S_{lk})/\mathrm{Re}(S_{lk})]$ were calculated. A peak of $C_{lk}(f)$ indicates synchronized oscillatory activity at the peak frequency f_{peak}, with a time delay $\tau_{lk} = \Delta\Phi_{lk}(f_{\mathrm{peak}})/(2\pi f_{\mathrm{peak}})$. We consider only $7 < f_{\mathrm{peak}} < 13$ Hz, and we use the terms time delay and phase difference interchangeably. It is worth mentioning that $\Delta\Phi_{l-k} = -\Delta\Phi_{k-l}$ and $-\pi < \Delta\Phi_{l-k} \leqslant \pi$. Directional influence from site l to site k was assessed via the Granger causality spectrum $I_{l\to k}(f)$ [21,23,71]. When the $I_{l\to k}(f)$ has a peak around f_{peak} obtained from the coherence spectrum, we consider that l G-causes k. In order to define back-to-front, lateral, or front-to-back influence we separated the electrodes in five lines [see Fig. 1(a)]: F_{P1} and F_{P2}; F_7, F_3, F_Z, F_4 and F_8; T_3, C_3, C_Z, C_4 and T_4; T_5, P_3, P_Z, P_4, and T_6; and O_1 and O_2.

[1] G. Buzsaki, *Rhythms of the Brain* (Oxford University Press, New York, 2006).
[2] X. J. Wang, Physiol. Rev. **90**, 1195 (2010).
[3] P. Fries, Trends Cogn. Sci. **9**, 474 (2005).
[4] A. Pikovsky, M. Rosenblum, and J. Kurths, *Synchronization: A Universal Concept in Nonlinear Sciences* (Cambridge University Press, Cambridge, 2001).
[5] S. M. Doesburg, A. B. Roggeveen, K. Kitajo, and L. M. Ward, Cerebral Cortex **18**, 386 (2008).
[6] E. Maris, T. Womelsdorf, R. Desimone, and P. Fries, Neuroimage **74**, 99 (2013).
[7] F. Varela, J. P. Lachaux, E. Rodriguez, and J. Martinerie, Nat. Rev. Neurosci. **2**, 229 (2001).
[8] J. Fell and N. Axmacher, Nat. Rev. Neurosci. **12**, 105 (2011).
[9] N. M. Dotson, R. F. Salazar, and C. M. Gray, J. Neurosci. **34**, 13600 (2014).
[10] G. G. Gregoriou, S. J. Gotts, H. Zhou, and D. R., Science **324**, 1207 (2009).
[11] P. H. Tiesinga and T. J. Sejnowski, Front. Human Neurosci. **4**, 196 (2010).
[12] A. M. Bastos, J. Vezoli, and P. Fries, Curr. Opin. Neurobiol. **31**, 173 (2015).
[13] M. S. Livingstone, J. Neurophysiol. **75**, 2467 (1996).
[14] E. Maris, P. Fries, and F. van Ede, Trends Neurosci. **39**, 86 (2016).
[15] A. Korzeniewska, M. Mańczak, M. Kamiński, K. J. Blinowska, and S. Kasicki, J. Neurosci. Methods **125**, 195 (2003).
[16] J. F. Marsden, P. Limousin-Dowsey, P. Ashby, P. Pollak, and P. Brown, Brain **124**, 378 (2001).
[17] D. Williams, M. Tijssen, G. van Bruggen, A. Bosch, A. Insola, V. D. Lazzaro, P. Mazzone, A. Oliviero, A. Quartarone, H. Speelman, *et al.*, Brain **125**, 1558 (2002).
[18] A. Schnitzler and J. Gross, Nat. Rev. Neorosci. **6**, 285 (2005).
[19] P. Sauseng and W. Klimesch, Neurosci. Biobehav. Rev. **32**, 1001 (2008).
[20] R. W. Thatcher, Develop. Neuropsychol, **37**, 476 (2012).
[21] A. Brovelli, M. Ding, A. Ledberg, Y. Chen, R. Nakamura, and S. L. Bressler, Proc. Natl. Acad. Sci. U. S. A. **101**, 9849 (2004).
[22] R. F. Salazar, N. M. Dotson, S. L. Bressler, and C. M. Gray, Science **338**, 1097 (2012).

[23] F. S. Matias, L. L. Gollo, P. V. Carelli, S. L. Bressler, M. Copelli, and C. R. Mirasso, NeuroImage **99**, 411 (2014).

[24] D. W. Hahs and S. D. Pethel, Phys. Rev. Lett. **107**, 128701 (2011).

[25] V. A. Vakorin, O. Krakovska, and A. R. McIntosh, in *Directed Information Measures in Neuroscience* (Springer, Berlin, 2014), pp. 137–158.

[26] L. Dalla Porta, F. S. Matias, A. J. dos Santos, A. Alonso, P. V. Carelli, M. Copelli, and C. R. Mirasso, Front. Syst. Neurosci. **13**, 41 (2019).

[27] F. Montani, O. A. Rosso, F. S. Matias, S. L. Bressler, and C. R. Mirasso, Phil. Trans. R. Soc. A **373**, 20150110 (2015).

[28] H. U. Voss, Phys. Rev. E **61**, 5115 (2000).

[29] C. Masoller and D. H. Zanette, Physica A **300**, 359 (2001).

[30] M. Ciszak, J. M. Gutiérrez, A. S. Cofiño, C. R. Mirasso, R. Toral, L. Pesquera, and S. Ortín, Phys. Rev. E **72**, 046218 (2005).

[31] K. Pyragas and T. Pyragienė, Phys. Rev. E **78**, 046217 (2008).

[32] G. Ambika and R. E. Amritkar, Phys. Rev. E **79**, 056206 (2009).

[33] C. Mayol, C. R. Mirasso, and R. Toral, Phys. Rev. E **85**, 056216 (2012).

[34] J. Sausedo-Solorio and A. Pisarchik, Phys. Lett. A **378**, 2108 (2014).

[35] M. Ciszak, O. Calvo, C. Masoller, C. R. Mirasso, and R. Toral, Phys. Rev. Lett. **90**, 204102 (2003).

[36] S. Sivaprakasam, E. M. Shahverdiev, P. S. Spencer, and K. A. Shore, Phys. Rev. Lett. **87**, 154101 (2001).

[37] S. Tang and J. M. Liu, Phys. Rev. Lett. **90**, 194101 (2003).

[38] M. Ciszak, C. R. Mirasso, R. Toral, and O. Calvo, Phys. Rev. E **79**, 046203 (2009).

[39] N. J. Corron, J. N. Blakely, and S. D. Pethel, Chaos **15**, 023110 (2005).

[40] K. Srinivasan, D. V. Senthilkumar, R. Mohamed, K. Murali, M. Lakshmanan, and J. Kurths, Chaos **22**, 023124 (2012).

[41] T. Pyragienė and K. Pyragas, Nonlin. Dyn. **74**, 297 (2013).

[42] T. Pyragienė and K. Pyragas, Nonlin. Dyn. **79**, 1901 (2015).

[43] A. Y. Simonov, S. Y. Gordleeva, A. Pisarchik, and V. Kazantsev, JETP Lett. **98**, 632 (2014).

[44] F. S. Matias, P. V. Carelli, C. R. Mirasso, and M. Copelli, Phys. Rev. E **84**, 021922 (2011).

[45] F. S. Matias, P. V. Carelli, C. R. Mirasso, and M. Copelli, PloS ONE **10**, e0140504 (2015).

[46] M. A. Pinto, O. A. Rosso, and F. S. Matias, Phys. Rev. E **99**, 062411 (2019).

[47] Y. Hayashi, S. J. Nasuto, and H. Eberle, Phys. Rev. E **93**, 052229 (2016).

[48] G. C. Dima, M. Copelli, and G. B. Mindlin, Int. J. Bifurcation Chaos **28**, 1830025 (2018).

[49] Y. Liu, Y. Takiguchi, P. Davis, T. Aida, S. Saito, and J. M. Liu, Appl. Phys. Lett. **80**, 4306 (2002).

[50] Y. Hayashi, J. Blake, and S. J. Nasuto, *Anticipation Across Disciplines* (Springer, Cham, 2016), pp. 275–282.

[51] N. Stepp and M. T. Turvey, Cogn. Syst. Res. **11**, 148 (2010).

[52] A. Washburn, R. W. Kallen, M. Lamb, N. Stepp, K. Shockley, and M. J. Richardson, PloS ONE **14**, e0221275 (2019).

[53] I. R. Roman, A. Washburn, E. W. Large, C. Chafe, and T. Fujioka, PLoS Comput. Biol. **15**, e1007371 (2019).

[54] A. Sharott, P. J. Magill, J. P. Bolam, and P. Brown, J. Physiol. **562**, 951 (2005).

[55] H. U. Voss, Phys. Rev. E **93**, 030201(R) (2016).

[56] H. U. Voss and N. Stepp, J. Comput. Neurosci. **41**, 295 (2016).

[57] H. U. Voss, Chaos **28**, 113113 (2018).

[58] C. M. Gray, P. Knig, A. K. Engel, and W. Singer, Nature (London) **338**, 334 (1989).

[59] P. R. Roelfsema, A. K. Engel, P. König, and W. Singer, Nature (London) **385**, 157 (1997).

[60] P. J. Uhlhaas, G. Pipa, B. Lima, L. Melloni, S. Neuenschwander, D. Nikolić, and W. Singer, Front. Integr. Neurosci. **3**, 17 (2009).

[61] R. Vicente, L. L. Gollo, C. R. Mirasso, I. Fischer, and G. Pipa, Proc. Natl. Acad. Sci. U. S. A. **105**, 17157 (2008).

[62] L. L. Gollo, C. Mirasso, O. Sporns, and M. Breakspear, PLoS Comput. Biol. **10**, e1003548 (2014).

[63] F. van Ede, S. Van Pelt, P. Fries, and E. Maris, J. Neurophysiol. **113**, 1556 (2015).

[64] R. Brette and A. Destexhe, *Handbook of Neural Activity Measurement* (Cambridge University Press, Cambridge, 2012).

[65] P. L. Nunez, R. Srinivasan, A. F. Westdorp, R. S. Wijesinghe, D. M. Tucker, R. B. Silberstein, and P. J. Cadusch, EEG Clin. Neurophysiol. **103**, 499 (1997).

[66] S. P. van den Broek, F. Reinders, M. Donderwinkel, and M. Peters, EEG Clin. Neurophysiol. **106**, 522 (1998).

[67] W. Klimesch, P. Sauseng, and S. Hanslmayr, Brain Res. Rev. **53**, 63 (2007).

[68] M. Aguilar-Domingo, Ph.D. thesis, University of Murcia 2013, http://hdl.handle.net/10201/35143.

[69] L. Barnett and A. K. Seth, J. Neurosci. Methods **223**, 50 (2014).

[70] H. Akaike, IEEE Trans. Automatic Control **19**, 716 (1974).

[71] H. Lütkepohl, *Introduction to Multiple Time Series Analysis* (Springer, Berlin, 1993).